(REFEREED RESEARCH)

EFFECT OF CURRENT ON POLYMER JET IN ELECTROSPINNING PROCESS

ELEKTİRİK AKIMININ ELEKTROSPUN POLIMER JETI UZERİNDEKİ ETKİSİ

Fatma YALÇINKAYA

Department of Nanotechnology and Informatics, Centre for Nanomaterials, Advanced Technologies and Innovation, Technical University of Liberec

Received: 26.09.2014 Accepted: 10.07.2015

ABSTRACT

System and process parameters play a major role in the production of fine bead free electrospun nanofibers. In this study, the influence of the system and process parameters were observed during the production of polyvinyl butyral (PVB) nanofibers. PVB nanofibers were produced by a needle electrospinning system. The voltage and feed rate of the system was varied to observe its effect on the electric current applied to a polymer jet. It was observed that the applied voltage and flow rate utilized on the polyvinyl butyral polymer solution affected the electric current's influence on the jet regimes (e.g. stable jet, fluctuated jet and stable jet with polymer drops). Nanofiber morphology showed the differences in fiber quality for each parameter. Additionally, the effect of conductivity on current and various jet regimes was examined. The properties of each of the samples were compared as parameters of the spinneret were varied in each experiment. The current test was used to determine if the surface morphology of the nanofiber was beadless.

Keywords: PVB, current, electrospinning, nanofiber, voltage.

ÖZET

Sistem ve işlem parametreleri elektro lif çekim yöntemiyle oluşturulmuş boncuksuz ve ince çaplı nanolifler üzerinde büyük rol oynamaktadır. Bu çalışmada sistem ve işlem parametrelerinin polyvinyl butiral (PVB) nanolifler üzerindeki etkisi çalışılmıştır. PVB nanolifleri elektro lif çekim yöntemi uygulanarak üretilmiştir. Farklı voltaj ve besleme hızı kullanarak jet üzerindeki akim ölçülmüştür. Uygulanan voltaj ve besleme hızının jet rejimlerinin (örn. Sabit jet, dalgalı jet ve polimer damlamalı sabit jet) oluşumda rol alan akimi etkilediği gözlemlenmiştir. Nanoliflerin morfolojisi her rejimde farklılık göstermiştir. Dahası iletkenliğin jet akimi ve farklı jet rejimleri üzerindeki etkisi incelenmiştir. Deneysel şartların sonucu olarak toplanan nanoliflerin özellikleri kıyaslanmıştır. Akim testi bocuksuz nanolif yüzeyinin tayini için kullanılmıştır.

Anahtar kelimeler: PVB, akim, elektro lif çekim yöntemi, nanolif, voltaj

Corresponding Author: Fatma Yalcinkaya, fatma.yalcinkaya@tul.cz

1. INTRODUCTION

Nanofibers have gained attention due to their uses in a variety of technological applications including but not limited to medical, filters, composites, sound absorption, electronics, absorbent, insulation, barriers, sensors, wipes, and personal care applications. There are several methods to produce nanofibers such as template synthesis, melt electrospinning, force spinning, bicomponent method, phase separation, electrospinning [1-7]. Electrospinning is a versatile method to produce very fine nano fibers.

The effects of parameters on the production of nanofibers have been studied for many years. Jet charge density is known as one of the most important parameters affecting the fiber diameter. It was found that when the charge density increases the fiber diameter decreases [8]. Deitzel et. al. studied the effect of the processing variables on the morphology of electrospun nanofibers and found that the onset of bead defect formation increased with current as the voltage was varied [9]. Theron et al. examined the influence of different process parameters on the electric current and volume and surface charge density in the polymer jet. They

also investigated and modeled multiple jets systems electrospinning polymer solutions [10, 11].

Shin et. Al. Found that net charge density appears to be related to the flow rate for high flow rates in PEO solution [12].

Majority of experimental data shows a power law relationship between solution flow rate (Q) and electric current (I) when the voltage is fixed [11,13, 14] as shown in Formula (1),

$$I \sim Q^{\alpha} \quad (1)$$

where α is the scaling exponent. When α=1 the relationship is isometric, and when ≠1 it is allometric [15, 16]. The value of the exponent α is dependent upon the solution.

Bhattacharjee et. al. demonstrated that the current I_{Total} is measured in electrospinning scales as (2)

$$EQ^{0.5}K^{0.4} \quad (2)$$

where E is electrical field, Q is feed rate, and K is conductivity for a wide variety of solutions in organic solvent [17].

In this report we observe the current that was measured and recorded in real time. Pokorny et. al. measured the current with an oscilloscope in order to understand the theoretical description of the electrospinning process [18].

Samatham et. al. studied the jet regimes and its effects on fibers formation. They found that morphology of polyacrylonitrile nanofibers are influenced by the jet regimes [19].

Herein, current was linked to flow rate of polymer solution and applied voltage. The Electric current while electrospinning was measured in real time while applying variable voltage and flow rate to PVB polymer solution. The effect of needle diameter on the electric current during the production of PVB fibers has been reported before [20]. In this work the effect of feed rates and applied voltage on the current was studied. It was observed that changes in current yielded to different jet regimes, which correlated with the fiber morphology. It was observed that current measurements can be used as key indicator to detect a bead-free fiber surface.

2. MATERIAL AND METHODS

Polyvinyl butyral (PVB) was purchased from Kuraray – the grade Mowital B 60 H (mol. Weight 60.000 g/mol). Ethanol was used to dissolve PVB. Zinc chloride ($ZnCl_2$) salt was purchased from Lachema. Conductivity (Radelkis OK-102/1), viscosity (Haake Roto Visco 1 at 23 °C), surface tension (Krüss K9) tests were performed at 24°C. SEM images were taken by Phenom FEI. Current tests were done with HP Hewlett Pack 34401A multimeter.

8% wt. PVB60H was prepared by adding 0.1% wt. $ZnCl_2$ ethanol mixture. All solutions were spun on a needle-electrospinning system (Fig. 1) in proper conditions as shown in Table 1. The current apparatus was connected to collector.

The electric current in the electrospinning process was determined by having an ohmic resistor (9841Ω) in series between the collector and the ground (Fig. 1). Electric current was calculated using Ohm's law.

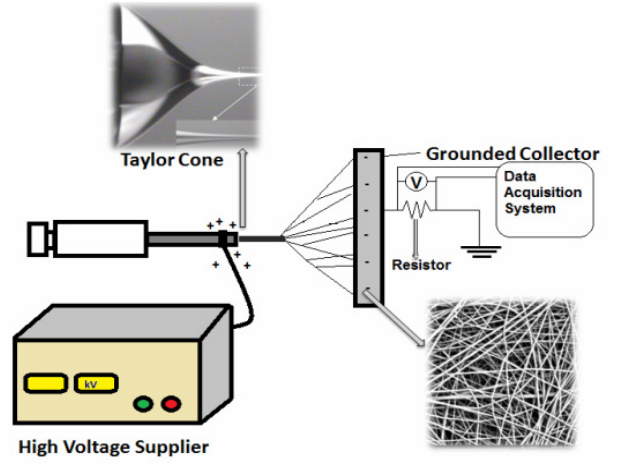

Figure 1. Diagram of needle-electrospinning system.

3. RESULT AND DISCUSSION

3.1. Solution Properties

Viscosity, surface tension and conductivity data was collected and tabulated in Table 2.

Table 1. Spinning Conditions of PVB polymer solution

Polymers	Applied Voltage(kV)	Distance Between Electrodes(mm)	Needle Dia. Outer/Inner (mm)	Feed Rate(mL/h)	Temp. (°C)	RH (%)
8% PVB 8% PVB+0.1% $ZnCl_2$	15-17-19-21-23-25	152	0.6/0.33	0.2-0.6-1.0	23	35

Table 2. Polymer solution properties

Polymers	Surface Tension (mN/m)	Cond. (mS/cm)	Viscosity (Pa.s)
8% PVB	23.5	0.016	0.0711
8% PVB+0.1% $ZnCl_2$	23.6	0.034	0.076

Table 2 clearly shows that additional salt did not affect the viscosity and surface tension. A possible explanation is the salt of complexing metal- $ZnCl_2$ may not be interacting with the macromolecules in the polymer solution, which gives reason to the stable viscosity. From literature we know that adding salt increases conductivity due to increasing the amount of ions in the solution. From previous work we also know that adding $ZnCl_2$ salt increased the spinnability of the PVB polymer solution due to its high conductivity [21].

According to the data we expect the average current of PVB with salt would be higher. A needle electrospinning system and memory oscilloscope were used simultaneously according to Figure 1. The effect of applied voltage and feed rate were examined. It was observed that current on the jet affected the jet regime, as a result the fiber morphology was affected. Three specific jet regimes were investigated.

3.2. Jet Regimes

a-fluctuating jet: polymer solution that reaches the end of the needle is immediately ejected as a jet, until the solution is depleted from the tip. When the jet reaches the collector, the electric current is observed and when the jet stops it pauses the circuit. The flow rate was maintained by a syringe pump, therefore polymer solution is repeatedly replenished. Because of the high electrical field applied, the above process take places frequently leading to a rapidly fluctuating jet [17, 20].

b-stable jet: electric current measured with stable jet.

c-stable jet with polymer drops: a jet forms until a drop is formed at the needle tip. It takes time to collect the drop. It is slow process of regime (a). After the drop falls from the tip of needle, another stable jet is formed.

The jet current was determined as a function of applied voltage and flow rate. From the data collected through the data acquisition and camera system in real time, it was concluded that there is a relationship between the jet regime and current. The graph in Figure 2 below explains the occurring process:

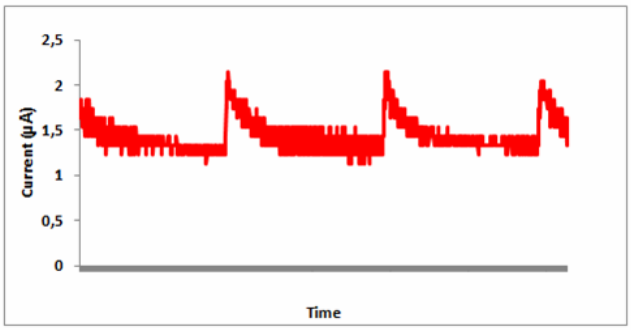

Figure 2. Current of stable jet with polymer drops.

It is evident from Fig. 2 that a jet forms at the needle tip and then is followed by the formation of a drop. Due to gravity, the drop of polymer solution falls, registering as a peak on the graph. Then the jet forms again repeating the cycle.

Current Graphs

The electric current data was graphed according to the results in various changes of the voltage and feed rate. Jet regimes were marked on the images. Figure 3, 4 and 5 displays the current recorded for the 8% wt. PVB polymer solution.

If the applied voltage is high and the feed rate is not sufficient, jets form and dissipate suddenly. This event continues cyclically as shown at 25 kV and 23 kV in Fig. 3, 4 and 5.

When the applied voltage is 21kV and 19 kV the jets showed characteristics of case a and b demonstrated in the graph in Fig. 3.

Increasing the feed rate to 0.6 mL/h yielded more a stable jet than a lower feed rate due to an adequate supply of the polymer solution for spinning. The acceleration time of the jet is equal to the feed rate between 15-19 kV. At 21 kV, the jet regimes demonstrated a more stable form instead of a fluctuating form. As a result both cases were observed at 21 kV in Fig. 4 and 5.

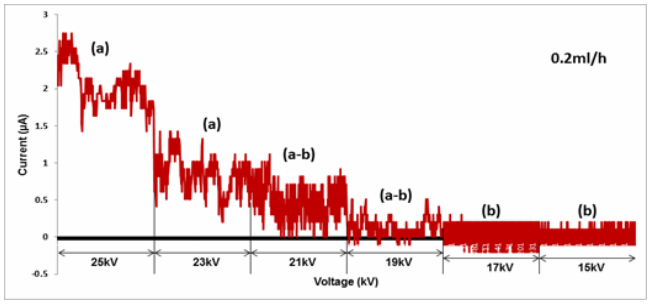

Figure 3. Current vs. Applied voltage with the feed rate 0.2 mL/h for 8% wt PVB solution.

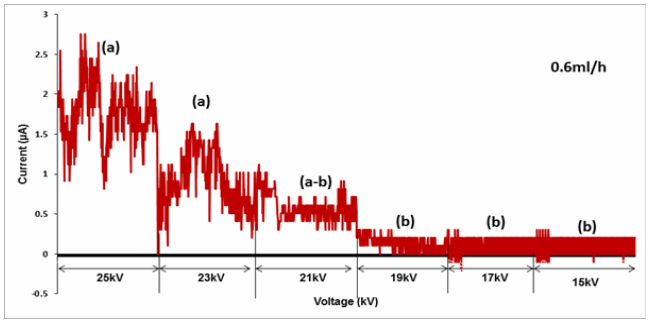

Figure 4. Current vs. Applied voltage with the feed rate 0.6 mL/h for 8% wt PVB solution.

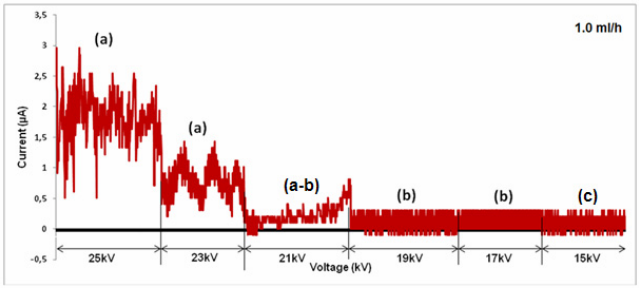

Figure 5. Current vs. Applied voltage with the feed rate 1.0 mL/h for 8% wt PVB solution.

In figure 5, the jets exhibited characteristics of case c at 15 kV. At the lowest applied voltage and the highest feed rate, the voltage is not sufficient to transport all the polymer solution to the collector. The remaining amount solution that

is not transported forms a droplet and falls as a result of gravity.

Figure 6, 7 and 8 show the result of currents for 8% wt. PVB+ 0.1% wt. $ZnCl_2$ polymer solution.

The jet regime observed spinning PVB with salt using the lowest feed rate (0.2 mL/h) exhibited fluctuating characteristics due to the feed rate not being sufficient.

Increasing feed rate provided more polymer solution to spin. As a result, the jets observed demonstrated more stable characteristics especially in 19, 17 and 15 kV as shown in Fig. 7. When the feed rate was increased to highest value (1.0 mL/h), we observed the stable jet case range was broader than using a lower feed rate as shown in Fig 8.

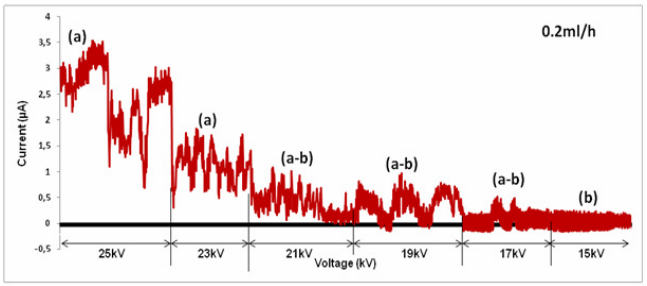

Figure 6. Current vs. Applied voltage with the feed rate 0.2 mL/h for 8% wt PVB+0.1% salt solution.

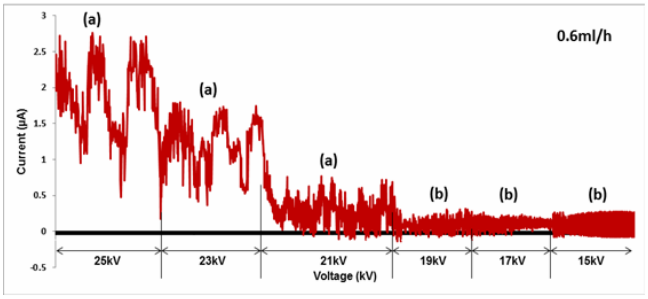

Figure 7. Current vs. Applied voltage with the feed rate 0.6 mL/h for 8% wt PVB+0.1% wt. salt solution.

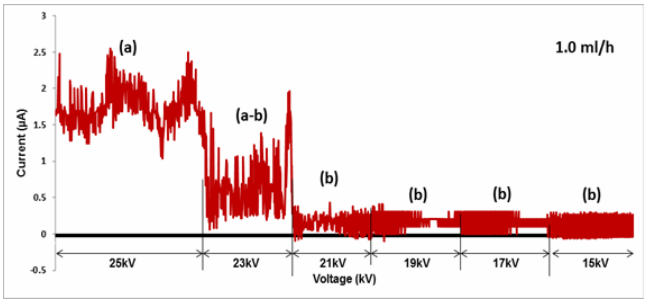

Figure 8. Current vs. Applied voltage with the feed rate 1.0 mL/h for 8% wt PVB+0.1% wt. salt solution.

From graphs we can see that average currents are approximate to each other when using solutions with and without salts while keeping the flow rate and the applied voltage consistent. However, the jet observed in the solution which has salt was more stable. It could be because of a higher conductivity due to a greater concentration of conductive ions which causes the drawn jet to be more stable.

The relationship between current, electrical field, conductivity and feed rate were calculated according to Formula 2 (Fig. 9).

Bhattacharjee et. al. observed a linear relationship between current and $E^*Q^{0.5}*K^{0.4}$ [17]. However, our results show that this relationship looks like parabolic than linear. It is evident that these parameters affect the data collected on electric current; however, we can hardly say that current scales with E, Q and K in case of PVB solutions. It could be because of the very low conductivity of PVB solutions compared to literature [17]. The relationship between jet regimes and the final fiber morphology were also investigated.

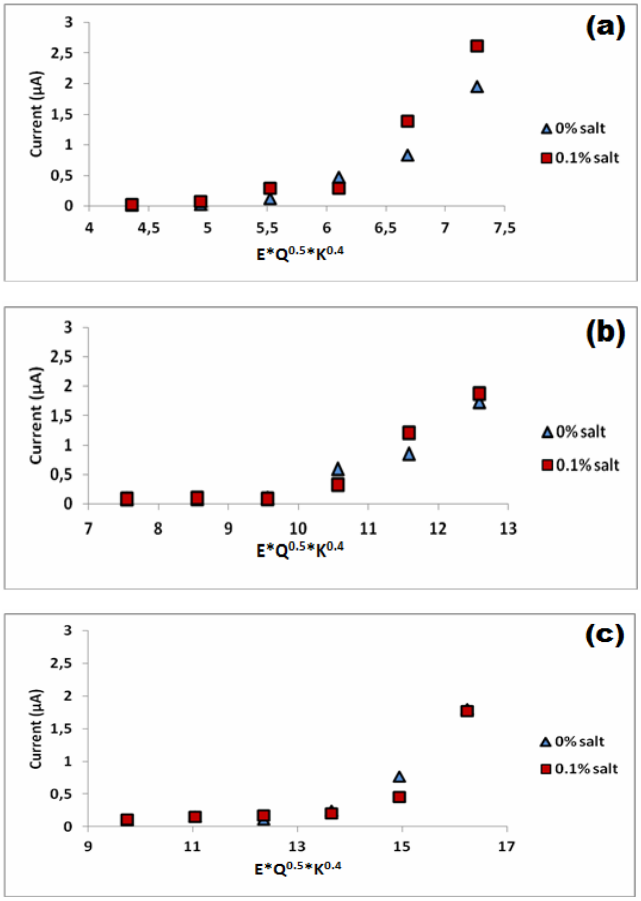

Figure 9. Plot of current vs. $E^*Q^{0.5}*K^{0.4}$, **(a)** at 0.2 mL/h, **(b)** at 0.6 mL/h, **(c)** 1.0 mL/h feed rate

3.3. Fiber Morphology

Current data showed that there were three kinds of jet regimes that could be effective on the fiber morphology. In the case of PVB solution without salt, these three jet regimes were observed and showed in Fig. 9.

Fig. 10. (a) shows the fluctuating jet regime when the feed rate and applied voltage was 1.0 mL/h and 25 kV respectively. Due to an unstable current, the resultant fibers have beads structure. The same result was observed in the case a-b at the 1.0 mL/h feed rate and 21 kV as shown in Fig. 10 (b). The more stable currents were exhibited in case b and c. The fibers produced displayed more uniform and bead free structure on the nonwoven web surface. Fig. 10 (c) and (d) were spun with the feed rate and applied voltages 1.0 mL/h and 17 kV and 15 kV respectively. The

case b and c has a more stable current graph than the other cases. The fiber diameter with a st. deviation and percentage of non-fibrous area was evaluated and tabulated in Table 3. The non-fibrous area indicates regions that are composed of beads or polymer droplets and fibers on the surface of fabric.

According to literature increasing the applied voltage decreases the fiber diameter until a limit [9, 22, 23]. Herein, the effect of voltage is easily visible.

PVB with salt solution had only three cases during spinning as shown in Fig. 11.

Herein we can say that the unstable current graph shows fibers with beads as shown in Fig. 11 (a) and (b). The fiber diameters and beads area were calculated and tabulated in Table 3. Fig. 11 (a) was spun with 1.0 mL/h feed rate at 25 kV, (b) was spun with 1.0 mL/h feed rate at 23 kV and (c) was spun with 1.0 mL/h feed rate at 21 kV. The average diameter with % CV and nonfibrous area were tabulated in Table 4.

Table 4. data showed that additional salt and voltage affects the resultant fiber morphology. By using current results we can assume the fiber surface morphology with or without beads.

Table 3. Fiber diameter and nonfibrous area of PVB solution without salt

Sample	Mean Fiber Diameter (nm)	CV (%)	Nonfibrous Area
Case a (Fig. 10-a)	316.344	26.48	2.4 %
Case a-b (Fig. 10-b)	298.162	30.25	1.9 %
Case b (Fig. 10-c)	318.027	30.70	0 %
Case c (Fig. 10-d)	295.55	26.45	0 %

Table 4. Fiber diameter and nonfibrous area of PVB solution with salt

Sample	Mean Fiber Diameter (nm)	CV (%)	Nonfibrous Area
Case a (Fig. 11-a)	304.821	29.61	3.3 %
Case a-b (Fig. 11-b)	315.087	31.03	2.1 %
Case b (Fig. 11-c)	317.66	28.92	0 %

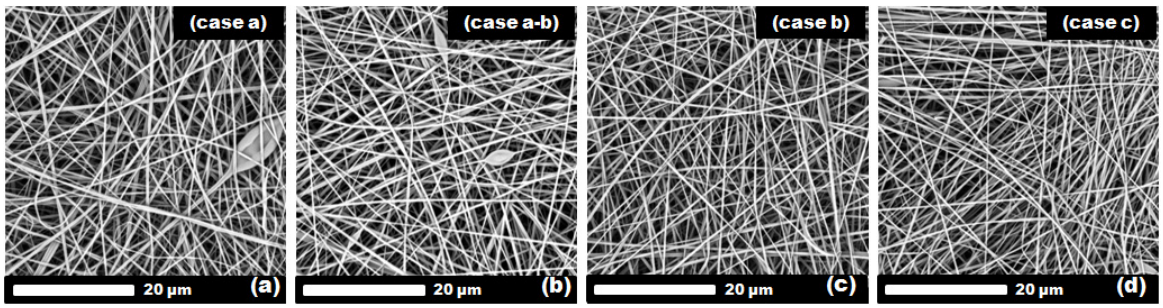

Figure 10. Various jet regimes of PVB polymer solution

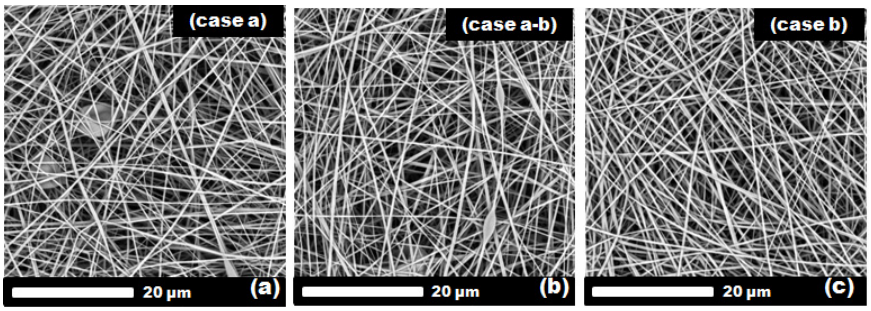

Figure 11. Various jet regimes of PVB+salt polymer solution

4. CONCLUSION

Using a new data collecting method while electrospinning can give useful information to help determine the formation of beads free fiber structures.

In this study, the current flowed on a jet was measured and graphed. The different behaviours of the electric current was observed and graphed.

The unstable graph data shows that the nanofibers have beads on the surface. Contrary, stable graphs (case b and c) represented beads free nanofibers. It was observed that structure and density of beads on the surface decreased with decreasing applied voltage.

PVB nanofiber with and without salt additive were used. By adding salt, the average current value did not change

significantly. Only jet regimes improved which exhibited beads free structures.

Using the Formula 2, the relationship between current, electric field, conductivity and feed rate was calculated and graphed. It seems that this relation is not linear as it was presented in literature [17] when a low conductive solution was used, PVB polymer solution showed different characteristics than other polymer solutions due to its low conductivity. Adding the salt improves conductivity slightly. The data of Figure 9 with and without salt did not create a linear relationship with current value.

As a result, it can be concluded that it is possible to control the formation of bead structures by using current test. Herein, the data shows current measurement can be a useful tool to detect beads free fibers during production for future applications. It is not possible to judge fiber diameter by using current measurement but it can be possible to detect a stable spinning process with bead free fibers. This test eliminates the extra effort and shortens the time needed to determine beads free nanofibers. By observing the electric current data, it will be possible to identify beads free nanofibers in a short amount of time. This method will shorten the time consuming in a needle electrospinning system.

In the future, this system can be design for industrial equipment for controlling stable spinning process.

ACKNOWLEDGEMENT

The authors are grateful to Baturalp Yalcinkaya and Prof. Oldrich Jirsak for their support. The results of this project LO1201 were obtained through the financial support of the Ministry of Education, Youth and Sports in the framework of the targeted support of the “National Programme for Sustainability I”.

REFERENCES

1. Ma P.X., Zhang R.Y., 1999, Synthetic nano-scale fibrous extracellular matrix, *J Biomed. Mater Res*, 46, 1, pp 60-72.
2. Fabbricante T.J., Fabbricante A.S., Ward G.F., Micro-denier nonwoven materials made using modular die units, *US patent 6114017 A, 2000*.
3. Huang T., Marshall L.R., Armantrout J.E., Yembrick S., Dunn W.H., Oconnor J.M., Mueller T., Avgousti M., Wetzel M.D., 2012, Production of nanofibers by melt spinning, *US patent 20080242171 A1*.
4. Torobin L., Findlow R.C., 2001, Method and Apparatus for Producing High Efficiency Fibrous Medin Incorporating Discontinous Sub-Micron Diameter Fibers and Web Media Formed Thereby, *US patent 6315806 B1*.
5. Pike R.D., 1999, Superfine microfiber nonwoven web, *US patent 5935883 A*.
6. Nain A.S., Wong J.C., Amon C., Sitti M., 2006, Drawing Suspended Polymer Micro/Nanofibers using Glass Micropipettes, *App. Phys. Lett*., 89, 18, pp 183105 - 183105-3.
7. Cengiz-Çallıoğlu F., 2014.'The Effect of glyoxal cross-linker and NaCl salt addition on the roller electrospinning of Poly(vinyl alcohol) nanofibers', Tekstil ve Konfeksiyon, 24(1), pp. 15-20
8. Fridrikh S.V., Yu J.H., Brenner M.P., Rutledge G.C., 2003, Controlling the fiber diameter during electrospinning, *Physical Review Letters*, 90(14).
9. Deitzel J.M., Kleinmeyer J., Harris D., Beck Tan N.C., 2001, The effect of processing variables on the morphology of electrospun nanofibers and textiles. *Polymer*, 42(1): p. 261-272.
10. Theron S.A., Yarin A.L., Zussman E., Kroll E., 2005, Multiple jets in electrospinning: experiment and modelin, *Polymer*, 46(9): p. 2889-2899.
11. Theron S.A., Zussman E., Yarin A.L., 2004, Experimental investigation of the governing parameters in the electrospinning of polymer solutions, *Polymer*, 45(6): p. 2017-2030.
12. Shin Y.M., Hohman M.M., Brenner M.P., Rutledge G.C., 2001, Experimental characterization of electrospinning: the electrically forced jet and instabilities, *Polymer*, 42(25): p. 9955-9967.
13. Demir, M.M., Yilgor I., Yilgor E., Erman B., 2002, Electrospinning of polyurethane fibers, *Polymer*, 43(11): p. 3303-3309.
14. He J.H., Wan Y.Q., Yu J.Y., Scaling law in electrospinning: relationship between electric current and solution flow rate, 2005, *Polymer*, 46(8): p. 2799-2801.
15. Kuikka J.T., 2002, Fractal analysis in medical imaging, *International Journal of Nonlinear Sciences and Numerical Simulation*, 3(2): p. 81-88.
16. Kuikka J.T., 2003 Scaling laws in physiology: Relationships between size, function, metabolism and life expectancy, *International Journal of Nonlinear Sciences and Numerical Simulation*, 4(4): p. 317-327.
17. Bhattacharjee P.K., Schneider T.M., Brenner M.P., McKinley G.H.,Rutledge G.C., 2010, On the measured current in electrospinning, *Journal of Applied Physics*, 107(4).
18. Pokorny P., Mikes P., Lukas D., 2010, Measurement of Electric Current in Liquid Jet, *Nanocon 2010, 2nd International Conference, Brno*, p. 282-286.
19. Samatham R., Kim K.J., 2006, Electric current as a control variable in the electrospinning process, *Polymer Engineering and Science*, 46(7): p. 954-959.
20. Yener F., Yalcinkaya B., Jirsak O., 2012, Effect of Jet Electric Current on Jet Regimes in Electrospinning of Polyvinyl Butyral Solutions, *in Fiber Society Conference*, *St. Gallen.*
21. Yener F., Jirsak O., 2011, Improving Performance of Polyvinyl Butyral Electrospinning, *Nanocon 2011, 3nd International Conference, Brno*, p. 356-361.
22. Jeun J.P., Lim Y.M., Nho Y.C., 2005, Study on morphology of electrospun poly (caprolactone) nanofiber, *Journal of Industrial and Engineering Chemistry*, 11(4): p. 573-578.
23. Wu C.M., Chiou H.G., Lin S.L., Lin J.M., 2012, Effects of electrostatic polarity and the types of electrical charging on electrospinning behavior, *Journal of Applied Polymer Science*, 126: p. E89-E97.